RSC Advances

PAPER

View Article Online
View Journal | View Issue

Cite this: *RSC Adv.*, 2025, **15**, 18158

Synthesis of rigid polyurethane foam from bio-based polyol obtained from microwave-assisted depolymerization of corn cob waste†

Florin-Marian Dîrloman, ‡[a] Aurel Diacon, ‡[ab] Oana Brincoveanu, [c] Gabriela Toader, [a] Miron Adrian Dinescu, [c] Ioan Calinescu, [b] Petre Chipurici, [b] Edina Rusen *[b] and Alexandra Mocanu *[bc]

Received 20th January 2025
Accepted 27th May 2025

DOI: 10.1039/d5ra00487j

rsc.li/rsc-advances

This study presents an innovative upcycling methodology for the production of rigid polyurethane (PUR) foams using a biopolyol (BioPol) synthesized from corn cob lignocellulose waste. The BioPol was obtained through microwave-assisted (MW) irradiation under acidic catalysis, followed by neutralization of the acidic medium. Rheological characterization of the lignocellulose-derived BioPol was conducted to evaluate its suitability for industrial applications. The PUR foam formulation was designed based on the hydroxyl number of the BioPol, as determined by ASTM D4274. BioPol was combined with a commercial trifunctional polyol derived from the oxypropylation of glycerol, enabling the entire polyol component of the formulation to be classified as bio-based. Increasing the BioPol content in the formulation enhanced the cross-linking density of the resulting foams, which also led to a reduction in the average pore diameter. Uniaxial compressive strength tests revealed superior mechanical properties, with maximum resistance recorded at 3.18 MPa compared with the blank sample. The resultant high-density rigid PUR foams exhibit excellent thermal stability, mechanical robustness, and ease of processability, establishing a promising pathway for developing durable and eco-friendly bio-based polyurethane products.

1. Introduction

Polyurethane products constitute nearly 8% of the global market, with current demand reaching 22.5 million tons being produced in several forms, depending on the final application as rigid, flexible, semi-rigid, fiber, elastomers, and adhesives.[1] The raw materials of polyurethane products consist of non-renewable diisocyanates and polyols, which present significant environmental challenges due to their reliance on fossil fuel-derived chemicals. This not only contributes to critical environmental issues but also raises serious concerns in terms of energy consumption and the production of non-biodegradable products.

Lignocellulose, derived from biomass such as wood or agricultural residues, offers a renewable and abundant, inexpensive source for polymer production compared to crude oil.[2] This trend has gained a lot of attention in the last decade, considering the worldwide struggle for building a cleaner environment while ensuring ecological methods for waste valorization or disposal.[3,4]

Valorization of lignocellulosic biomass involves the breakdown of the structure by several chemical processes necessary to separate the constituent components, such as cellulose, hemicellulose, and lignin.[3] The intrinsic composition of lignocellulose-based waste materials, comprising cellulose (9–80%), hemicellulose (10–50%), and lignin (5–35%), requires various pretreatment methods, whether physical, chemical, or biological, to enable the effective separation of its components.[5] Acidic or enzymatic hydrolysis can be applied to catalyze the breakdown of the cellulosic part into glucose or other sugars[6,7] which is then followed by a fractional process to separate the multitude of components/fractions of the biomass.[8]

The resulting constituents, cellulose and lignin-based fractions, can be separated by different techniques like filtration, centrifugation, solvent extraction, precipitation, or membrane processes.[9–11] All these pretreatment, processing, and separation steps include sometimes the use of harsh conditions like

[a]*Military Technical Academy "Ferdinand I", 39-49 George Coșbuc Boulevard, 050141 Bucharest, Romania*

[b]*National University of Science and Technology Politehnica Bucharest, Faculty of Chemical Engineering and Biotechnologies, 1-7 Gh. Polizu Street, 011061 Bucharest, Romania. E-mail: edina.rusen@upb.ro*

[c]*National Institute for Research and Development in Microtechnologies – IMT Bucharest, 126A Erou Iancu Nicolae Street, Voluntari, Ilfov, 077190, Romania. E-mail: alexandra.mocanu@imt.ro*

† Electronic supplementary information (ESI) available. See DOI: https://doi.org/10.1039/d5ra00487j

‡ Florin-Marian Dîrloman and Aurel Diacon will be considered as first authors with equal contribution.

high pressures and temperatures, the use of hazardous chemicals, or can be time-consuming processes.[8]

Lignin is an amorphous polyol mainly constituted of three phenolic monomers connected through carbon–carbon or etheric bonds: *p*-coumarol, coniferyl alcohol, and sinapyl alcohol, being difficult to break down into low-molecular-weight compounds.[12,13] The polyols production from depolymerized fragments of lignocellulose can be achieved through different processes such as hydroxymethylation, liquefaction, oxypropylation, and phenolation.[1,13–15]

Regardless of the lignocellulose biomass processing method liquid polyols obtained from agricultural waste processing have three primary advantages: (i) their physical and chemical properties are comparable to those of their petrochemical counterparts;[13] (ii) they offer environmental protection benefits through waste processing into new products; (iii) they support circular economy by designing bio-based and biodegradable products.[14,16–18]

When considering the different agricultural waste available, corncobs residue represents a very appealing alternative, considering it represents up to 14% of the 1163 million tons of maize produced in 2022.[19] Corncob waste valorization routes are very extensive[20] including the production of animal feed,[21] compost,[22] biofuels,[23] biochar,[24] specialty chemicals,[25] nanocomposites, biopolymers[26] and others.[27]

Polyurethane foams are incredibly versatile materials[28] due to their unique properties and uses[29] such as structural components[30] (due to their good mechanical resistance, thermal resistance, and thermal insulation), furniture and automotive parts[31] (due to control over density and flexibility), adhesives[32] (due to their strong bonding and sealing properties), molded parts[33] and other customized applications.[34] One of the current stress points in polyurethane foams research involves the development of green formulations through the exploitation of biomass-derived biopolyols.[35]

In this study, we propose a two-stage process involving (1) the depolymerization of corncob waste by glycerol microwave-assisted glycolysis and (2) the direct use of the obtained biopolyol (BioPol) without further separation to produce rigid polyurethane foams.

When assessing the proposed strategy against the 12 Principle of Green Chemistry[36] at least 8 principles are fulfilled: (1) atom economy is achieved (the BioPol product was entirely integrated into the polyurethane rigid foam formulation); (2) designing safer chemicals (the synthesis methods are designed to use and generate chemicals and products that possess little or no toxicity to human health and the environment, respectively bio-based polyols and polyurethane rigid foams); (3) design for energy efficiency (energy consumption reduction by using microwave irradiation at ambient pressure with a shorter reaction time); (4) renewable feedstock is used (corncob waste); (5) reduce derivatives (the glycolysis process applied to obtain BioPol does not require the use of additional reagents for protecting groups and it is obtained in one-pot reaction); (6) catalysis (the strategy is based on the use of several catalyzed steps for shorter reaction time); (7) design for degradation (the corncob waste is degraded by glycolysis process to obtain bio-based environmentally friendly polyol and polyurethane foams); (8) inherently safe chemistry for accident prevention (the processes do not involve harsh/dangerous reaction conditions). This approach is based on the experience gained in our previous research[37] involving the development of polyurethane adhesive formulations using polyols from the solvolysis of birch wood lignocellulose biomass. However, for this study, a more sustainable biomass source was selected to give an alternative to valorize the corn cob waste, which in our country is generally used for ignition, compost, and animal feed. Over the past two decades, corn stover and corn cobs have been the most extensively utilized biomass resource in second-generation (2G) biorefineries, and the production of bio-based chemical compounds is the most abundant globally, surpassing both wheat and rice straw agricultural residues in availability.[38] In addition, the polyols production process by acidic catalyzed glycolysis was intensified using microwave irradiation to reduce the depolymerization reaction time.

This innovative process design has been adopted due to its advantages, which include a more efficient thermal control, reduced energy consumption (due to shorter processing time), increased lignocellulose conversion into biopolyols (BioPol), lower production costs of biopolyols compared to conventional processes, and removal of additional separation steps. The recovered liquid fraction was included in the formulation of rigid polyurethane foams together with a commercial bio-derived triol polyether-polyol derived from oxypropylation of glycerol (PETOL 56-3). The polyurethane foams were obtained in closed metallic molds without the use of any blowing agents or additives to maintain a greener formulation of the final products.

This study demonstrates a new advanced approach toward fully bio-renewable polyol systems, demonstrating that even the precursors used in the synthesis of PETOL 56-3 can be derived from sustainable, renewable sources. To the best of our knowledge, this is also the first study in which high-density rigid polyurethane foams produced *via* glycolysis of corn cobs were obtained – an unprecedented achievement in valorizing agricultural waste.

2. Materials and methods

2.1. Materials for foam formulations

The lignocellulose biomass consisted of corncob obtained from agricultural processes in Giurgiu County, Romania. The corncobs were grinded, sieved, and the fraction with less than 500 μm was utilized in the glycolysis procedure. Prior to the glycolysis process, the corncobs fraction was dried to 5% wt moisture content. Glycerol (99%, Sigma-Aldrich, Germany), sulfuric acid H_2SO_4 (96% wt) (Sigma-Aldrich, Germany), H_3PO_4 (85%, Sigma-Aldrich, Germany), acetone (Merck, Romania), tetrahydrofuran (THF) (Sigma-Aldrich, Germany), NaOH flakes (reagent grade 97%, Merck, Romania) were used as such for the synthesis, separation and purification of corn-based polyol. Polyether-polyol-based on glycerol PETOL 56-3 (hydroxyl index, $I_{OH} = 53 \div 59$ mg KOH per g, Chimcomplex S.A. Borzești, Romania), 4,4′-diphenylmethane-diisocyanate (MDI, –NCO content = 30.5 ÷ 32.5%, Covestro Desmodur® 44V20L, Merck,

Romania), 2,6-toluene diisocyanate (TDI, –NCO content = 30.5 ÷ 32.5%, Covestro Desmodur® T80, Merck, Romania) and triethanolamine (TEOA, ≥99% (GC), Sigma-Aldrich, Germany) were used without further chemical interventions in the design process of the foams formulations.

2.2. Methods

2.2.1. Synthesis of glycolysis product from corn cob lignocellulose biomass (BioPol). In a 10 L reactor fitted with microwave generator (3 quartz windows – one at the bottom and 2 side-by-side windows for three 800 W microwave generators, with a maximum use of power use of 50%), 500 g of finely ground corncob waste (d < 500 μm) were added in 5000 g glycerol. After reaching 190 °C, a mixture of H_2SO_4 and H_3PO_4 (1 : 1 molar ratio, 2 wt% *versus* the reaction mixture) was added, and the reaction was stirred mechanically (200 rpm) under nitrogen atmosphere in a microwave field at constant temperature (190 °C). After 2 h reaction time, the mixture was neutralized using NaOH flakes by slow addition under stirring until a neutral pH was reached. A 500 g sample was taken from the reactor at the end of the process and diluted with a mixture of THF : water (v/v) (4 : 1). The unreacted biomass was recovered by filtration, followed by drying to constant mass to establish the conversion value (96.1%). After vacuum evaporation to remove

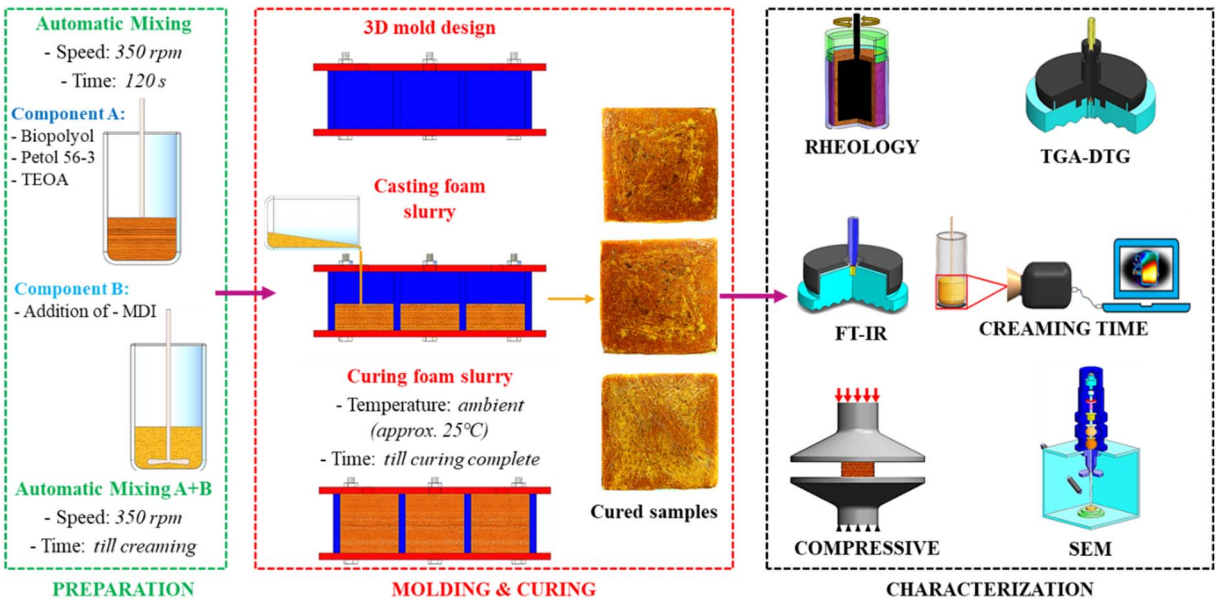

Scheme 1 Schematic representation of the development and characterization of foam formulations.

Table 1 The composition of the developed foam specimens[a]

Sample	Composition	BioPol : PETOL 56-3 weight ratio	Aspect and curing time
SP563	MDI : PETOL 56-3 + TEOA[b] (212 g PETOL 56-3, 1 g TEOA + 36.67 g MDI)	—	Compact structure; CT[c] = 96 h
SP9-3M	MDI : BioPol + PETOL 56-3 + TEOA[b] (115 g BioPol, 38.3 g PETOL 56-3, 1 g TEOA + 95.2 g MDI)	9 : 3	Crumbly surface, non-homogeneous aspect; CT[c] = 48 h
SP7-5M	MDI : BioPol + PETOL 56-3 + TEOA[b] (95 g BioPol, 67.86 g PETOL 56-3, 1 g TEOA)	7 : 5	Compact structure; CT[c] = 72 h
SP5-7M	MDI : BioPol + PETOL 56-3 + TEOA[b] (73 g BioPol, 102.2 g PETOL 56-3, 1 g TEOA + 84.98 g MDI)	5 : 7	Compact structure; CT[c] = 84 h
SP5-7T	TDI : BioPol + PETOL 56-3 + TEOA[b] (80 g BioPol, 112 g PETOL 56-3, 1 g TEOA + 56.26 g TDI)	5 : 7	Compact structure; CT[c] = 96 h

[a] Each formulation was demonstrated at a 250 g scale for reproducibility, each square of the mold being filled with the same amount of formulation after creaming time was reached. [b] 0.4% catalyst reaction (TEOA), as weight percentage calculated from the total weight of the binder. [c] Curing time (CT).

water traces (<0.3%), the liquid BioPol was used for characterization procedures, namely hydroxyl number, FT-IR analysis, and rheological properties. The rest of the product inside the reactor was separated in the same way to obtain the BioPol, which was further used to design the rigid bio-based polyurethane foams.

2.2.2. Synthesis of polyurethane foams based on biopolyols from corncob. The manufacturing of polyurethane foams is depicted in Scheme 1. Organic mixtures were prepared in different weight ratios of 9 : 3, 7 : 5, and 5 : 7 between BioPol : PETOL 56-3 while keeping a molar ratio of 1.3 between –NCO/–OH groups using TEOA as catalyst and reaction agent (detailed in Table 1).

A Nahita DJ-1 mechanical stirrer was used to mix component A (BioPol with PETOL 56-3) and component B (the diisocyanate) in a polypropylene beaker at room temperature (about 25 °C) at a speed of 350 rpm until the working time ("creaming time") was reached. The resulting mixtures were poured into a closed metallic mold (with a polyethylene coating of the walls) with three cubic compartments (Scheme 1) and allowed to cure at room temperature.

The resulting foam samples were removed from the metal compartments of the mold and processed according to specific analyses, as detailed in the following characterization section.

3. Characterization of the developed foam samples

3.1. Determination of hydroxyl number for biopolyols (I_{OH})

To ensure a constant ratio (1.3) between the –NCO and –OH groups, the formulations of the polyurethane foams were based on the hydroxyl number. The I_{OH} of the biopolyols resulting from the glycolysis reaction was determined using the standard test methods for testing polyurethane raw materials: determination of hydroxyl numbers of polyols – ASTM D4274-method D as described in the ESI.†

3.2. Rheological characterization of component A

Using a coaxial cylinder viscometer, Rheotest 2 (Medingen GmbH, Germany), outfitted with a rotating cylinder "H" designed for fluids with high viscosities, the fluid flow characteristics for the bio-based polyols and component A were determined at a temperature of 25 °C. The Ostwald-de-Waele model, also known as the power law fluid, was used to determine the rheological parameters based on eqn (1) and apparent viscosity, $\mu_{app,}$ as a function of shear rate by eqn (2):

$$\tau = m\left(\frac{\partial u}{\partial y}\right)^{n} \quad (1)$$

$$\mu_{app} = m\left(\frac{\partial u}{\partial y}\right)^{n-1} \quad (2)$$

in which τ is the shear stress (Pa), m is the flow consistency index (Pa s^n), $\frac{\partial u}{\partial y}$ is the shear rate (also referred to as $\dot{\gamma}$) (s^{-1}), and n is the flow index (dimensionless). According to our previous work,[39] the readings that fell within a deviation of 1% necessary to determine the shear stress were recorded after 30 seconds, required for the stabilization of the measurement. The rheological measurements resulted from the variation of shear rate while registering α parameter which was expressed as the shear stress by multiplying its value with the geometrical value, Z, attributed for each rotational cylinder ($Z = 6.26$ for cylinder S2 – samples PETOL 56-3, and component A-5-7; $Z = 28.9$ for cylinder H – samples BioPol and component A-7-5). The result of the mathematical multiplication of α and Z was divided by 10 to express shear stress in Pa.[40]

3.3. FT-IR characterization of bio-based polyurethane foams

FT-IR spectra of the PUR foams and the raw materials were obtained using a Spectrum Two FT-IR spectrometer (PerkinElmer, MA, USA). Small discs were cut from the foam specimens, and droplets of liquid components were used for analysis. Spectra were collected in transmission mode with a resolution of 4 cm^{-1}, in the range 4000–550 cm^{-1}, where the main characteristic peaks of mixtures and organic components are found. An accumulation of 32 scans, to obtain an acceptable signal-to-noise ratio, was taken within this interval.

3.4. Density determination of the bio-based polyurethane foams

The density of the blank polyurethane foam (SP563) and the formulated samples (SP5-7M, SP7-5M, SP5-7T, and SP9-3M) were determined using ASTM D7710-14 – The Standard Test Method for Determination of Volume and Density of Rigid and Irregularly Shaped Molded Cellular Materials. The density was determined by dividing the mass by the volume of each sample. Each PUR sample was cut into a cube shape with a side of 25 mm and weighed to find the mass. For precise determination, the mass measurements were performed using an analytical balance with 5 decimals (AUW220D, Shimadzu, 5 decimals). To determine the volume for each sample, a graduated cylinder was filled with water to a certain level, after which the sample was submerged at the bottom of the vessel. The difference between the new level and the initial level was registered as the volume. The test was conducted in triplicate, and the density expressed as kg m^{-3} was calculated for each sample. The average density, and the average squared deviation, were detailed in Table 2.

3.5. Structural characterization and determination of pore size distribution

The structural characterization of all polyurethane specimens was obtained with a Nova NanoSEM 630 Scanning Electron

Table 2 Density values for developed foam samples

Sample	Average density (kg m^{-3})	Standard deviation
SP563	508	2.4
SP5-7T	571	1.9
SP5-7M	587	1.7
SP7-5M	589	4.7
SP9-3M	593	324.4

Microscope (FEI Company, Hillsboro, OR, USA) at an acceleration voltage of 10 kV. To increase the resolution of the micrographs, all samples were sputtered with a thin layer of Au of a few nanometers. By measuring about 100 individual pores, the pore size distribution of the formulated specimens was statistically obtained from SEM micrographs. The Gauss function provided the best match for the histograms, which showed a unimodal distribution of the pores.

3.6. Thermogravimetric analysis of bio-based polyurethane foams

The thermogravimetric analysis (TGA-DTG) was carried out by a thermogravimetric apparatus model Netzsch TG 209 F3 Tarsus (NETZSCH, Selb, Germany). Each sample mass (approximately 4 mg) was heated under nitrogen atmosphere from 25 to 900 °C, at a heating rate of 10 °C min^{-1}.

3.7. Determination of creaming time

Creaming time or pot working time for the analyzed foam suspensions was determined according to our previous work[37] using a FLIR A6700 MWIR infrared camera under the following conditions: sample amount: approximately 50 g; standard device temperature range: −15 °C to 90 °C. The mixture was stirred at a speed of 350 rpm with a mechanical mixer. The tests were carried out at ambient temperature till complete curing of the reaction.

3.8. Compression tests of the bio-based polyurethane foams

An Instron 68TM-50 Series universal testing instrument equipped with a 50 kN cell was used to perform mechanical compressive testing on cubic samples with a side of approximately 70 mm, at a strain rate of 2.38×10^{-4} s^{-1}. The tests were conducted at ambient temperature.

4. Results and discussion

4.1. Hydroxyl number of polyols

The first step of this study consisted in the determination of the hydroxyl number, I_{OH}, for the biopolyol resulted from the glycolysis of corncob wastes using the standard method ASTM D4274 – method D. The I_{OH} was determined to be 260 mg KOH per g, as calculated using eqn (1) and the detailed procedure provided in the ESI† based on ASTM D4274.

4.2. Rheology analysis of raw materials and component A

The following step involved the rheological characterization of component A, given that scaling up the synthesis process is crucial in the industrial sector since the PUR products are obtained by various methods that need high stirring rates for total homogenization of component mixtures.

Fig. 1 indicates the rheological behavior by plotting the shear stress (Pa) as a function of the increasing shear rate (s^{-1}) of PETOL 56-3 (Fig. 1a), BioPol (Fig. 1b) and both formulations for

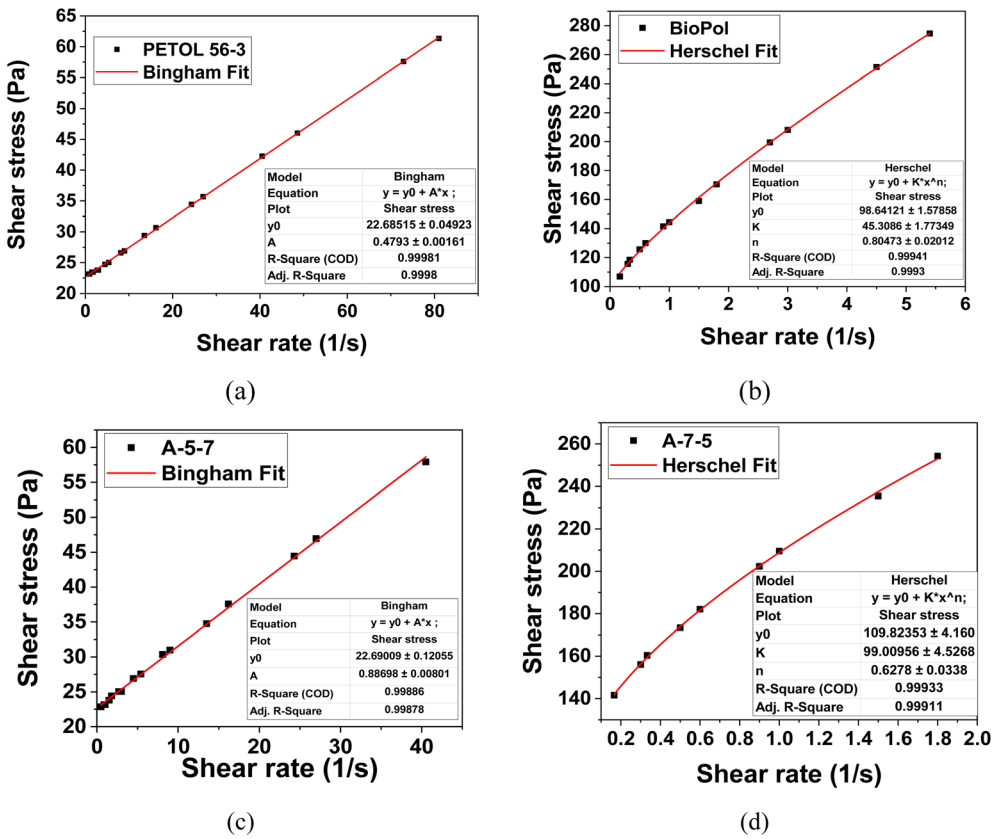

Fig. 1 The shear stress (Pa) *vs.* shear rate (s^{-1}) plots of PETOL 56-3 (a), BioPol (b), component A-5-7 (c), and component A-7-5 (d).

component A (Fig. 1c and d) before the reaction with MDI or TDI.

The Bingham fluid behavior of the PETOL-56-3 polyol was shown in Fig. 1a. This indicates that to cause the fluid to flow, a shear stress, y_0, of 22.68 ± 0.049 Pa must be applied. After exceeding this value, the PETOL-56-3 fluid has a Newtonian rheological behavior, signifying that the viscosity of the fluid is directly proportional to the deformation represented by shear rate.[41,42]

The shear stress-shear rate plotted for the BioPol sample (Fig. 1b) resulted from the depolymerization of corncobs fitted best to the Herschel model[41] since the value of R^2 was close to unity, registering a value of 0.99941. In the ESI (Fig. S1†), the data were plotted against linear (R^2 = 0.8122, Fig. S1a†) and Bingham model (R^2 = 0.99449, Fig. S1b†) to prove that the Herschel model fits best our results. The Herschel type of fluid flow is a non-Newtonian fluid characterized by three parameters: the proportionality or consistency k (Pa s^n), the flow index n (dimensionless), and the yield shear stress, y_0 (Pa).[43] It is worth mentioning that the k parameter is assigned to m, and the shear stress y is assigned to τ as mentioned in the theoretical part (Section 3.3). The parameter n indicates how strongly a fluid exhibits shear-thickening behavior ($n > 1$) or shear-thinning behavior ($n < 1$), while y_0 represents the stress threshold that must be exceeded before the fluid begins to flow.[43]

In this study, below the value of y_0 of 98.64 ± 1.57 Pa, the BioPol sample will behave like a solid, and above this value will have a fluid-like characteristic. Additionally, given that the n parameter was less than 1, the BioPol had a shear-thinning characteristic based on the registered value for n (0.8 ± 0.02).

The ratio between PETOL-56-3 and BioPol in the mixtures affected the rheological characteristics of the two resultant A components. Every A component showed traits similar to PETOL-56-3 or the BioPol, the dominant polyol determining the rheological resemblance (Fig. 1c and d). Thus, the A component with the highest concentration of PETOL-56-3 (component A-5-7) indicated a Bingham fluid behavior, registering a value of 22.69 ± 0.12 Pa of the yield stress (Fig. 1c). Above this value, component A-5-7 will exhibit a Newtonian fluid rheological behavior.[41,42] On the other hand, in Fig. 1d, component A-7-5 indicated a similar behavior with the BioPol, being a Herschel fluid with a yield stress value y_0 of 109.82 ± 4.16 Pa, and with shear-thinning characteristic n of 0.62 ± 0.03. To reinforce our results, the BioPol rheological behavior similar to the Herschel model fluid fits literature data in which similar behavior was registered for biopolyols obtained from glycerol liquefaction of cellulose biomass.[44]

4.3. FT-IR analysis of raw materials and polyurethane foam specimens

To confirm the efficient reaction between the mixture of the two polyols and the curing agents, FT-IR analysis was performed on the raw materials and the PUR components as described in Table 1. The results are illustrated in Fig. 2.

The broad signal recorded at 3314 cm^{-1} corresponds to the –NH groups present in the structure of PUR-designed foams and

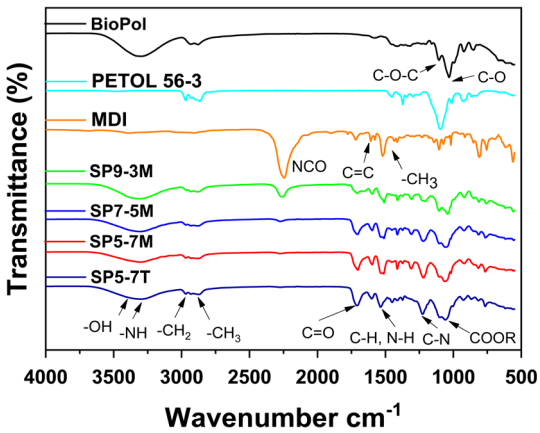

Fig. 2 FT-IR transmittance spectra of BioPol (BioPol), commercial polyol (PETOL 56-3), curing agent (MDI), and developed foam specimens (SP9-3M, SP7-5M, SP5-7M, and SP5-7T).

to the –OH from the absorbed water molecules, while the peaks at 2962 cm^{-1} and 2855 cm^{-1} correspond to the stretching vibration of the $-CH_2$ and $-CH_3$ groups within the same compounds.[45,46]

The characteristic vibration of the C=C group can be observed at 1582 cm^{-1}, which is characteristic for the aromatic rings of the isocyanate-based curing agents (MDI and/or TDI).[47] At 1504 cm^{-1} the band characteristic for the stretching vibration of the $-CH_3$ groups in triethanolamine, respectively MDI[47] can be noticed. Also, the intense signal at 2253 cm^{-1}, can be assigned to the –NCO group vibration.[37]

The signal at 1049 cm^{-1} can be associated with the vibrations of the C–O stretching group after breaking the glycosidic groups from the cellulose structure, being specific to the BioPol product resulting from the biomass degradation.[37,48] The ether C–O–C asymmetric stretching group at 1102 cm^{-1} is also specific to biomass degradation, as a result of lignocellulose depolymerization.[48] The ether group is also found in the structure of the commercial polyether polyol PETOL 56-3.

In the case of all the designed PUR foam specimens, the signal present at 1510 cm^{-1} was assigned to the bending vibration of the amide group N–H, which confirms the reaction between polyol and isocyanate reactants.[37] The signal at 1703 cm^{-1} is specific to the C=O elongation vibration, which supplementary confirms the formation of urethane groups resulting from the reaction between –OH groups (from the polyol component) and isocyanate (coming from MDI or TDI).[49] Another element that confirms that the reaction took place is the peak registered at 1230 cm^{-1} associated with the C–N bond.[49]

4.4. Density determination of the bio-based polyurethane foams

The values calculated for the density of the samples and the average squared deviation are presented in Table 2 (see Table S1† with a detailed version of density measurements in the ESI†). The density of the formulated PUR foams increases as the PETOL 56-3 content decreases, which can be attributed to the

presence of small, multifunctional OH-containing molecules in BioPol derived from cellulose degradation that promote a more compact and rigid structure through an increased number of cross-linking sites.[50] According to literature data,[51] high-density polyurethane foams register densities in the range of 550–650 kg m^{-3}. Thus, judging by the average density values from Table 2, the bio-based PUR formulations from this study fall into the rigid high-density foam category.[52] However, it is worth mentioning that in the case of sample SP9-3M, although the average density value was 593 kg m^{-3}, this value resulted from highly dissimilar values (see Table S1†). This could be an indication of the non-homogeneous structure of this specimen, which was also confirmed by organoleptic observation of the samples presented in Fig. S2† from the ESI.†

4.5. Structural characterization and determination of pore size distribution

The next step of this study involved conducting a morphological analysis of all the formulated specimens. SEM analysis, as illustrated in Fig. 3, revealed a highly porous structure for sample SP563 (blank sample). Various examined areas (Fig. 3a and b – 100×) exhibited a combination of large and small pores. However, at higher magnification (Fig. 3c – 1000×), it is worth mentioning that the wall structure of the blank PUR foam appeared compact.

The addition of BioPol component resulted from the depolymerization of lignocellulose biomass from corn cob waste led to a higher density of pores for SP5-7M specimen, as shown by Fig. 3d and e. Furthermore, at 1000×, the aspect of the PUR foam is much more porous (Fig. 3f) compared to the blank sample, the walls of the macropores being porous as well. This may be attributed to a higher reactivity of the lower molecular weight polyols contained in the BioPol polyol mixture.[53]

Changing the curing agent from MDI to TDI in SP5-7T formulation led to a porous structure in which larger or smaller pores with irregular shapes formed, compared to previous samples, as depicted in the two different areas that were investigated by SEM (Fig. 3g and f – 100×). Larger magnification (Fig. 3i – 1000×), however, revealed few pores with irregular shapes compared with previous samples (marked by the white circles). This behavior can be attributed to the higher reactivity of TDI compared with MDI, which can also lead to an increase in the reaction temperature and rate.[54]

By increasing the concentration of the BioPol in component A, specimen SP7-5M registered a porous structure in which larger pores alternate with smaller pores (Fig. 3j and k) and the walls of the macropores have a compact aspect similar to the blank sample (Fig. 3l).

Considering that the purpose of this study was to design fully PUR bio-based foams, the next step involved the use of a higher concentration of lignocellulose-derived BioPol. However, the content of BioPol used for the PUR formulation of SP9-3M specimen led to a non-homogeneous aspect at a macroscopic level, as presented in Fig. S2† – ESI,† also confirmed at a smaller scale by SEM analysis. Fig. 3m, respectively, Fig. 3n indicated the formation of some large irregular pores/holes, while the detailed image (Fig. 3o) showed large irregular cavities in which no pores were formed. This morphological aspect of SP9-3M is in good agreement with the anomalies that were registered for the density values presented in Section 4.4.

To compare the pore size distribution for samples SP563, SP5-7M, SP5-7T, SP7-5M, and SP9-3M, the data were obtained from SEM images by measuring around 100 individual pores. The software "Image J" was used to extract the necessary information from the SEM micrographs and compile the histograms. Table 3 summarizes the values obtained from the "Image J" program, while the histograms are presented in Fig. S3† from the ESI.†

In the case of using BioPol in sample SP5-7M, the mean pore diameter (160 ± 76 μm) was lower compared with the blank sample (320 ± 101 μm), SP563. By increasing the BioPol concentration in sample SP7-5M, the mean pore diameter slightly decreased to 144 ± 65 μm. The highest concentration of BioPol in sample SP9-3M led to a significant decrease of the mean pore diameter, which indicates that by increasing the bio-based polyol content, a reduced mean pore diameter is registered. This can be correlated with the BioPol content that increases in the order SP5-7M, SP7-5M, and SP9-3M, determining a higher viscosity of the reaction mixture that is correlated with reduced pore diameter due to an increased resistance to pore growth.[55] Additionally, by replacing MDI with TDI, in the same composition, the pore size range was smaller as well as the mean diameter of the pores for sample SP5-7T compared with SP5-7M, indicating that at higher reactivity of component B, the mean pore diameter of the pores decreased. Additionally, SEM statistical analysis confirmed that by increasing the BioPol content, a decreased mean size diameter of the pores (Table 3) was registered, being correlated with higher density (Table 2) of the bio-based foams, which is in good agreement with literature data[56] (Fig. S4† – ESI†).

4.6. Thermogravimetric results of bio-based polyurethane foams

The thermal stability of polyurethane products is important for their applications and temperature domain utilization. Thus, the next step of this study involved the determination of the TG curve (Fig. 4a), and the respective DTG curve (Fig. 4b) as a function of temperature ranging from room temperature to 900 °C.

Table 4 presents the significant weight losses observed at different temperatures for the considered polyurethane foam samples and the polyol raw materials (PETOL 56-3 and BioPol). The PETOL 56-3 registered a two-step weight loss process, the first step with an onset at 185 °C (and a maximum at 206 °C) while the second has an onset at 250 °C (and a maximum at 336 °C) and a residual mass below 1% being registered at temperatures above 600 °C. For the BioPol sample a three-step weight loss process was also observed with the first having an onset at 115 °C and a maximum at 222 °C followed by a second step both of them corresponding to 80% weight loss while the last degradation stage corresponds to a weight loss of 7% and has an onset at 670 °C. The complex thermal decomposition process

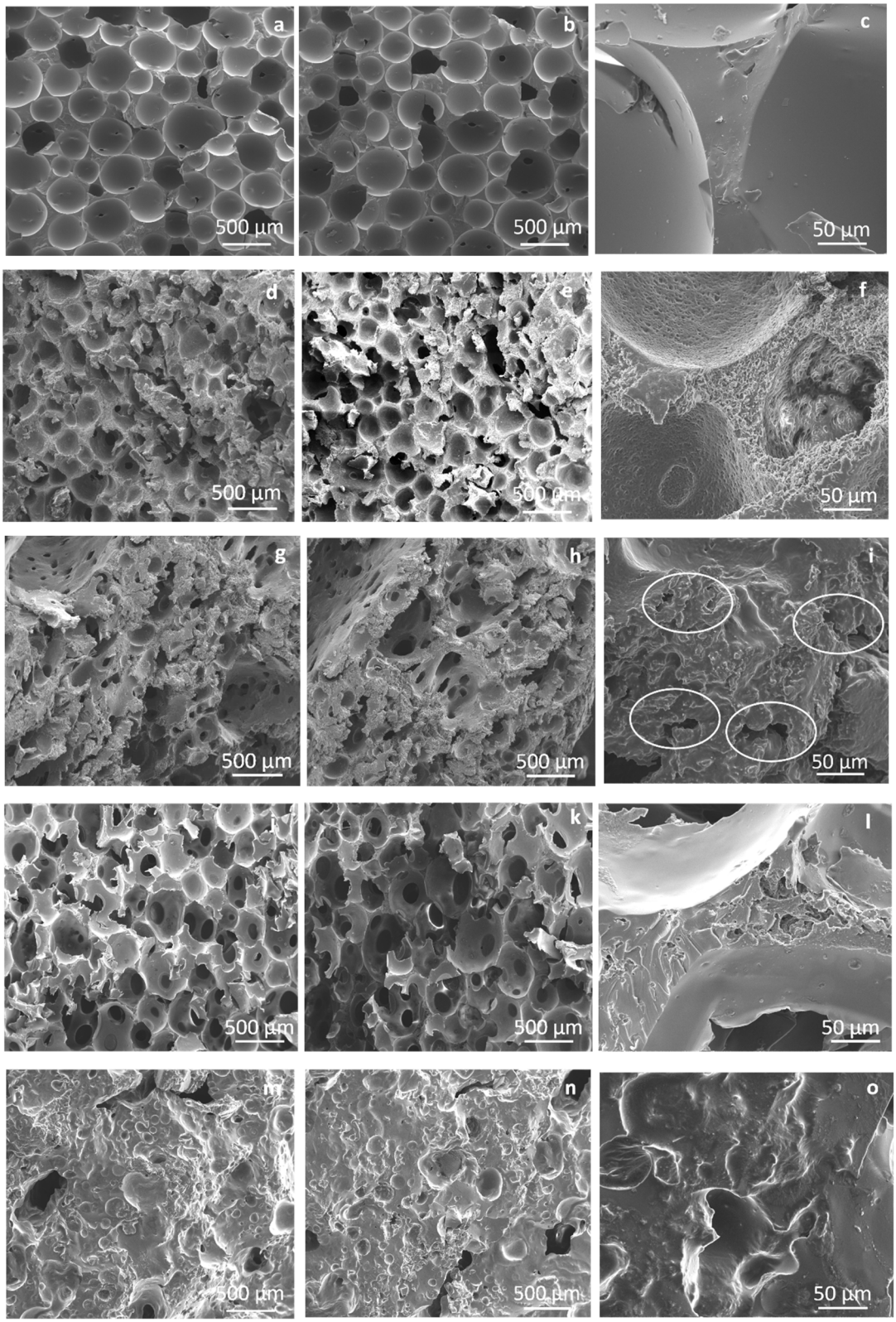

Fig. 3 SEM micrographs performed in different areas of the PUR specimens at two different magnifications for SP563 (a and b – 100×; c – 1000×), SP5-7M (d and e – 100×; f – 1000×), SP5-7T (g and h – 100×; i – 1000×), SP7-5M (j and k – 100×; l – 1000×), SP9-3M (m and n – 100×; o – 1000×).

Table 3 The values obtained for pore size range, pore size range with the highest percentage, and mean pore diameter

Sample code	Pore size range (μm)	Pore size range with the highest percentage (μm)	Highest percentage (%)	Mean size diameter (μm)
SP563	104 ÷ 577	220 ÷ 418	66.3	320 ± 101
SP5-7M	34 ÷ 381	64 ÷ 177	66.6	160 ± 76
SP7-5M	65 ÷ 381	67 ÷ 183	85.1	144 ± 65
SP9-3M	19 ÷ 372	35 ÷ 116	80.4	76 ± 49
SP5-7T	11 ÷ 249	40 ÷ 133	81.2	88 ± 49

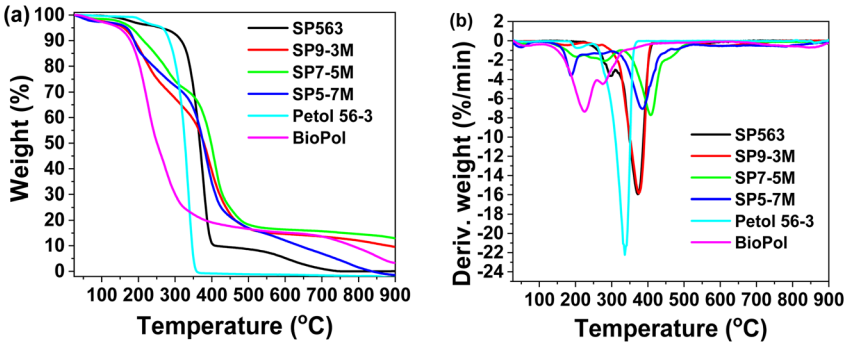

(a) (b)

Fig. 4 (a) TG and (b) DTG profiles of polyurethane foam samples.

of polyurethanes can be directly connected not only with soft and hard segments from the polyurethane structure itself, but also with small molecular weight compounds resulting from the depolymerization of lignocellulose. Thus, the discussion for the thermal degradation of the samples is focused on the most significant weight loss stages. Accordingly, decomposition for the blank sample occurs in three stages from room temperature to 200 °C (I), from 300 to 400 °C (II), and from 400 to 900 °C (III). The first decomposition step of the blank sample, SP563, indicated approximately 3.3% weight loss, likely due to surface-adsorbed moisture. The most significant weight loss (89.07%) occurred between 300 and 400 °C (Fig. 4 and Table 4), being associated with the decomposition of urethane groups and reformation of alcohols, isocyanate, amines, olefines, and carbon dioxide,[57] while after 700 °C, the sample is completely degraded.

In the case of all samples based on BioPol, up to 200 °C, the weight loss was significantly higher compared with that of the blank sample which could be attributed to a higher hydrophilicity due to a larger number of OH groups and degradation of the crosslinked domains involving lower molecular weight species, degradation of the diisocyanate-based hard segments.[57,58] The second significant degradation step occurred for all bio-based products from 300 to 400 °C, being attributed to the degradation of the urethane group and soft segments consisting of polyols, sample SP5-7M registering the highest weight loss at 400 °C (64.5%) (Table 4). By increasing the BioPol content, sample SP7-5M registered the lowest weight loss (51.2%) at 400 °C (Fig. 4b and Table 4), thus being the most stable sample in terms of temperature degradation. However, the formulation that had the highest BioPol content, SP9-3M, registered almost the same weight loss value at 400 °C as the sample with the lowest BioPol content this being attributed to the anomalies obtained for this sample in terms of stirring, non-uniform macroscopic aspect (Fig. S2† – ESI†) and density values, and statistical pore size values as discussed before. Thus, compared with the blank sample, samples SP7-5M and SP5-7M were the most thermally stable at

Table 4 The decomposition process of foams at different temperature values

	Weight loss [%]							
Sample	200 °C	300 °C	400 °C	500 °C	600 °C	700 °C	800 °C	900 °C
SP563	3.29	7.47	89.07	91.33	94.82	98.99	99.97	99.98
SP9-3M	12.47	32.35	63.36	83.17	85.39	86.37	87.96	90.38
SP7-5M	7.81	25.56	51.24	81.72	83.65	84.32	85.94	87.05
SP5-7M	13.33	27.45	64.52	82.97	87.84	92.97	98.38	99.97
PETOL 56-3	3.29	7.47	89	91.4	94.82	99	99.97	100
BioPol	18.22	69.93	80.87	83.43	84.85	86.35	90.98	96.7

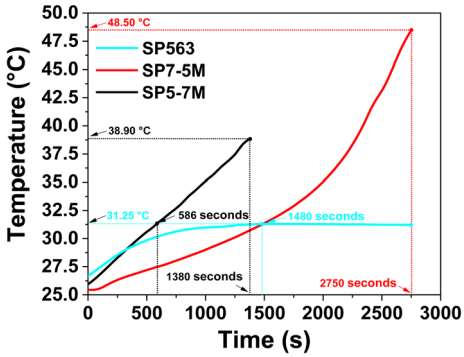

Fig. 5 Temperature *versus* curing time profiles during continuous stirring of the foam formulations.

400 °C, the bulk decomposition being almost complete after 500 °C, while sample SP7-5M registered the highest residual mass at 900 °C (almost 13%).

4.7. Determination of creaming time

Creaming time, also known as gel time or the time from mixing to creaming in PUR foams, refers to the point at which the uniform mixture of component A, component B, and additives transforms into a creamy consistency and begins to expand. This period is crucial in foam processing because it marks the start of foam formation. Whether using injection, compression molding, or cast molding, the creaming time provides the small-scale user or industrial worker with a limited period to handle the stirred mixture. Once the expansion or rising starts, the mixture becomes more viscous and harder to process.

To determine in a more accurate form the creaming time, the temperature *versus* curing time profiles of the mixtures of the selected PUR foam formulations were registered (Fig. 5). For the next part of this study, we chose to investigate further samples SP5-7M and SP7-5M, based not only on their thermal properties but also on the density and organoleptic properties (demonstrated in ESI – Fig. S2 and Table S1†) of SP9-3 that proved non-homogeneous.

Thus, Fig. 5 illustrates the temperature increase from room temperature up to 50 °C during stirring, plotted as a function of the curing time, in comparison to the blank sample SP563. To reinforce the findings presented in Fig. 5 and Fig. 6 provides images captured by the infrared camera at three different stages, showing the temperature of the mixtures during stirring until gel-time was reached, as previously presented in another study.[37]

Sample SP563 registered a slight increase in temperature from room temperature to 31.25 °C at 1480 seconds (almost 25 minutes) (Fig. 5 – turquoise line), which constitutes the gel time (the moment at which the change in viscosity was clear as shown by the infrared camera – Fig. 6b). As the reaction continued with the rising step, the temperature remained constant for a period of up to 2750 seconds (almost 46 minutes) until no further foam expansion was observed by the camera.

In contrast, sample SP7-5M, although it had a gradually temperature increase up to 30.44 °C until 1480 seconds, registering the same creaming time as the blank sample (Fig. 5 – red line, Fig. 6e), sharply rised its temperature to 48.13 °C at 2750 seconds (Fig. 5, and Fig. 6f). This behavior can be explained by the higher content of BioPol, composed of reactive degradation products with small molecular weights that cause an increase of the reaction rate. For sample SP5-7M, a lower creaming time

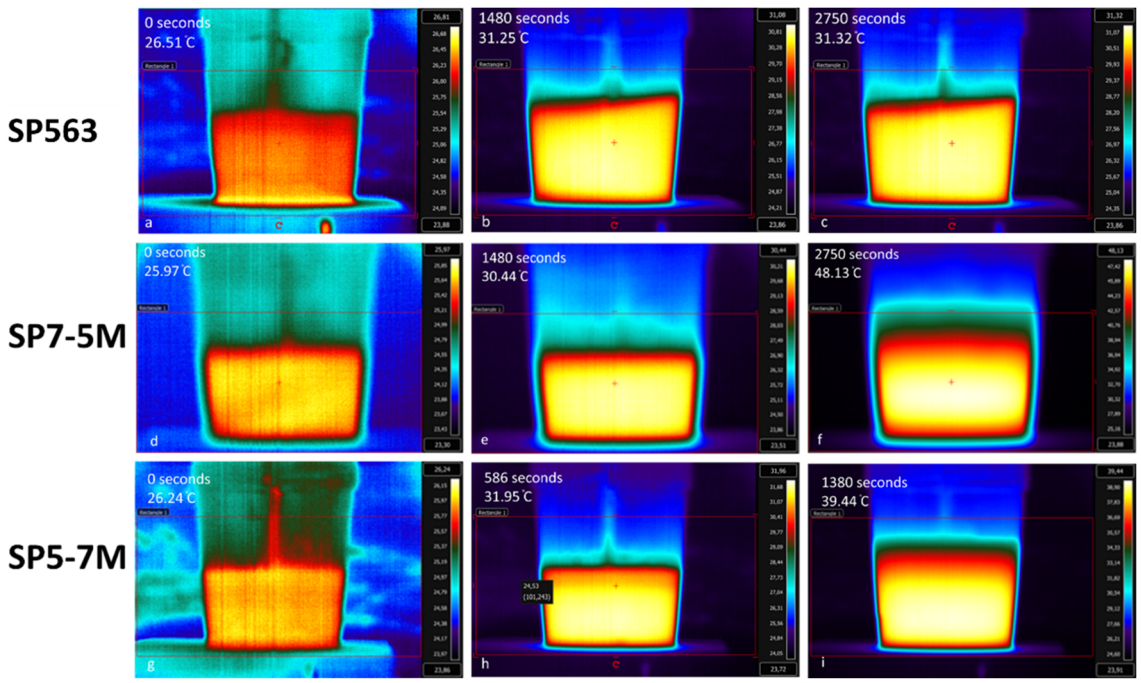

Fig. 6 Slurry behavior of foam mixtures at different time moments for blank sample SP563 (a–c), sample SP7-5M (d–f), and sample SP5-7M (g–i).

compared with all the other samples was registered after a gradual temperature rise, up to 31.95 °C of almost 10 minutes (Fig. 5 – black line, Fig. 6h). In this case, the rising time reached up to 1380 seconds (Fig. 6i), attaining a lower temperature compared with the sample with higher BioPol content (sample SP7-5M). This lower creaming time could be attributed to a lower viscosity compared to SP7-5M (see Fig. 1), while the number of OH groups involved in the reaction is higher than SP563 and lower than SP7-5M. Thus, lower viscosity facilitates homogenization, while the presence of more OH groups lead to higher temperatures.

4.8. Compression analysis of the PUR bio-based foams

Compressive testing is essential for assessing how formulation components influence the mechanical strength of polyurethane foams and the structural integrity of the final product. Thus, a uniaxial compressive test (Fig. S5†) was performed to evaluate the mechanical properties of the PUR foam formulations, and the results obtained are illustrated in Fig. 7. Fig. S5† indicates that each sample was analyzed in triplicate and measured before the compression test, while after the compression test, the aspect of the two BioPol-based foams was presented as an example.

As can be observed from the comparative graph in Fig. 7 and also from Table 5, the formulation identified as blank sample, SP563, displayed the lowest mechanical resistance, leading to significantly reduced compressive stress values compared to the other formulations. Conversely, the sample identified as SP7-5M demonstrated a significantly greater resistance to compressive stress, although it rapidly reached a plateau region specific for rigid foam structures that likely indicates the failure of the cellular structures.[59] Therefore, increasing the BioPol weight ratio resulted in samples exhibiting a significantly enhanced capacity to withstand compressive loading, but an excessively high concentration of lignocellulose-derived biopolyol could occasionally contribute to the formation of brittle structures. It is worth mentioning that the compression results for sample SP9-3M were not depicted in Fig. 7 since the data were not reproducible for foams with higher BioPol content.

The mechanical behavior of SP7-5M is likely attributable to its more compact porous structure, characterized by alternating larger and smaller pores, with the walls of the macropores

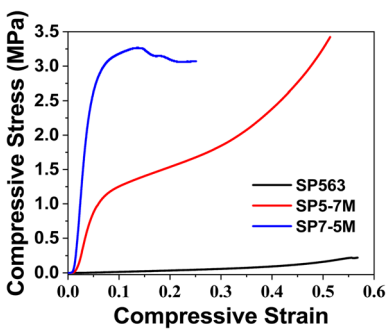

Fig. 7 Compressive stress–strain profiles for the PUR foam specimens.

Table 5 Compressive strain–stress values of the composite PUR foam formulations

Sample	Compressive strain (%)	Compressive stress (MPa)	Standard deviation (MPa)
SP563	10	0.0143	0.0005
SP5-7M		1.2525	0.08
SP7-5M		3.1823	0.15

displaying a compact aspect similar to the blank sample, as was observed by SEM analysis (Section 4.5 – Fig. 3l compared with Fig. 3c). The high stress values obtained for SP7-5M may be related to the increased content of compounds with a higher number of hydroxyl functionality and with lower molecular weights present in the lignocellulose-derived BioPol obtained by glycolysis, which led to a more rigid structure. Additionally, the higher pore size observed in the SP5-7M specimen (as described in Section 4.5), which exhibited a significantly more porous structure including porous walls of the macropores, resulted in greater flexibility compared to the SP7-5M sample. To be more specific, the compressive stress–strain for SP5-7M is specific for elastoplastic foams, with three compression stages as defined in literature data, as elastic, plastic, respectively densification stage, without the interference of a brittle stage and failure occurring in the plastic stage.[60]

Thus, the linear elastic region, marked by the bending of the foam cell walls, can be observed up to a strain of approximately 10%. Beyond this point, the slope of the curve decreases, likely due to the buckling and partial collapse of the cell walls. Once most of the cells have collapsed, further strain results in the compression of the solid polyurethane, leading to a sharp rise in the stress–strain curve. At this stage, the material densifies, forming a compacted foam structure. As a result, stress increases rapidly with further strain, with the stiffness of the compacted foam nearing that of the solid polymer. At a compressive strain of 10%, the highest compressive strain was registered by sample SP7-5M, which was 200 times higher compared with the blank sample (Table 5), while for sample SP5-7M, the increase was 87 times higher than the blank sample.

The comparative data presented in Table 6 highlight the diversity of biomass sources and synthesis strategies employed for the production of bicomponent rigid PUR foams. Most literature reports focus on bicomponent rigid PUR foams with lower densities ranging from 39 to 160 kg m^{-3} and corresponding compressive strengths below 1 MPa.[44,61–63]

In contrast, the rigid bicomponent PUR foams developed in this study using corn cob as lignocellulose-based waste demonstrate significantly higher density values ranging from 571 to 589 kg m^{-3}, accompanied by exceptionally high compressive strength, 1.25–3.18 MPa.

This positions the current materials as high-density, high-performance PUR foams, representing a notable progress over previously reported biomass-derived systems. The combination of a microwave-assisted biopolyol synthesis route and optimized foam formulation (without using blowing agents)

Table 6 Assessment of the density and compressive strength of the formulated PUR foams relative to PUR rigid foams obtained from biomass-derived biopolyols in prior studies

Type of biomass	Synthesis conditions	Type of product	Density, kg m^{-3}	Compressive stress, MPa	Reference
Corn stover	(1) Organosolv pre-treatment to remove lignin (2) Oxypropylation of lignin with propylene oxide and glycerol (2 h, 150 °C, 1 MPa)	Bicomponent rigid PUR	70 ÷ 130	0.1 ÷ 0.82	Li *et. al.*[61]
Kraft pine lignin	(1) Drying of lignin for 24 h (2) Liquefaction in glycerol and 1,4-butanediol (microwave assisted – 5 min, 180 W, 130 ÷ 170 °C, no catalyst)	Bicomponent rigid PUR	83 ÷ 150	0.62 ÷ 0.85	Gosz *et. al.*[62]
Cotton	(1) Drying up to 5.4% moisture (2) Liquefaction of cellulose cotton in glycerol (6 h, 120 ÷ 150 °C, acid catalyst)	Bicomponent rigid PUR	39 ÷ 42	0.26 ÷ 0.36	Kosmela *et. al.*[44]
Mixed biomass residues (digested sewage sludge, hemp stalk hurds, and sugar beet pulp)	(1) Drying at 105 °C for 24 h (2) Liquefaction in glycerol (acid catalyst step – 1 h, 110 ÷ 130 °C; base catalyst step – 45 min, 170 °C, nitrogen atmosphere)	Bicomponent rigid PUR	43 ÷ 160	0.03 ÷ 0.25	Jasiūnas *et. al.*[63]
Corn cob waste	(1) Drying up to 5% moisture (2) Solvolysis in glycerol (microwave assisted – 2 h, 190 °C, acid catalyst)	Bicomponent high-density PUR	571 ÷ 589	1.25 ÷ 3.18	This study

contributes to the mechanical superiority of the foams, highlighting the novelty and potential applicability of the developed materials in demanding structural or insulation applications.

5. Conclusions

In conclusion, this study successfully demonstrated the feasibility of producing rigid polyurethane foam starting from BioPol obtained *via* the depolymerization of lignocellulose biomass from lignocellulose corncob wastes, using acidic catalysis with glycerol under microwave irradiation. The lignocellulose-derived biopolyol (BioPol) was utilized in the formulation of rigid polyurethane foams with PETOL 56-3, a commercial homopolymer derived from the oxypropylation of glycerol. Therefore, the entire content of polyols involved in the formulations can be considered as from bio-renewable sources. Several polyol mixtures were prepared in different weight ratios of 9 : 3, 7 : 5, and 5 : 7 between BioPol and PETOL 56-3, while for the preparation of the foam, a molar ratio of 1.3 (between –NCO/–OH groups) was maintained. Also, TEOA was employed as a catalyst/crosslinker. The results showed that the rheology and the "creaming time" were influenced by the ratio between PETOL 56-3 and BioPol, while FT-IR analysis confirmed the complete reaction between the polyol components, curing agent, and catalyst. The density of the polyurethane foams is dependent on the BioPol content which facilitate the formation of a more compact and rigid structure due a higher number of cross-linking sites. The SEM analysis indicated that an increase in the BioPol component ratio led to a change in the morphology of the foam and of the density of the pores. Samples SP7-5M and SP5-7M were the most thermally stable at 400 °C, with SP7-5M having the highest residual mass at 900 °C, as confirmed by TGA analysis. The uniaxial compressive tests indicated that SP7-5M had higher stress values, likely due to the higher crosslinking density, due to the polyfunctional lower molecular weight polyols contained in the BioPol, leading to a more rigid structure. In contrast, the higher pore density in SP5-7M resulted in greater flexibility.

The developed approach not only highlights the potential for entirely bio-based polyol content but also underlines the feasibility of sourcing precursors from renewable sources, offering a sustainable and cost-effective production of high-density rigid PUR foams.

Data availability

The data supporting this article have been included as part of the ESI.†

Author contributions

Conceptualization, F. M. D., A. Diacon, E. R. and A. M.; methodology, G. T., A. Diacon and E. R.; validation, F. M. D., A. D., G. T., and A. M., I. C.; formal analysis, F. M. D., P. C., G. T., O. B., A. Dinescu and A. Diacon; investigation, F. M. D., A. Diacon, A. Dinescu, E. R., G. T., O. B., and A. M.; resources F. M. D., I. C. and A. D.; writing—original draft preparation, F. M. D., A. D., G.

T., and A. M.; writing—review and editing, F. M. D., A. M., G. T., I. C., P. C., E. R., and A. M.; supervision G. T., E. R. and A. M.; project administration, I. C., E. R., G. T. and A. D.; funding acquisition, G. T. and A. M. All authors have read and agreed to the published version of the manuscript.

Conflicts of interest

The authors declare no conflict of interest.

Acknowledgements

The authors acknowledge the financial support received from the Competitiveness Operational Program 2014–2020 Priority Axis: research, technological development, and innovation (RDI) in support of economic competitiveness and business development operation stimulating the demand of enterprises for innovation through RDI projects carried out by enterprises individually or in partnership with R&D institutes and universities in order to innovate processes and products in economic sectors that have growth potential, project title "Greenol-Biopolyols obtained through an unconventional technology of vegetal waste recovery", project code: 122990. A. Diacon acknowledges the financial support provided by the Executive Agency for Higher Education and Innovation Funding (UEFISCDI), the Ministry of Education of Romania, through the National Project PN-IV-P7.1-PTE2024-0486 ctr. no. 1PTE/2025. IMT team would like to thank for financial support in part by the Romanian Ministry of Research, Innovation, and Digitization through the Core Program within the National Research, Development and Innovation Plan 2022–2027, under Project 2307 – μNanoEl, contract number 8N/03.01.2023 and project "National Platform for Semiconductor Technologies", contract no. G 2024-85828/390008/27.11.2024, SMIS code 304244, co-funded by the European Regional Development Fund under the Program for Intelligent Growth, Digitization, and Financial Instruments.

References

1 M. H. Tran and E. Y. Lee, Production of polyols and polyurethane from biomass: a review, *Environ. Chem. Lett.*, 2023, **21**(4), 2199–2223.
2 X. Ge, C. Chang, L. Zhang, S. Cui, X. Luo, S. Hu, Y. Qin and Y. Li, Chapter Five - Conversion of Lignocellulosic Biomass Into Platform Chemicals for Biobased Polyurethane Application, in *Advances in Bioenergy*, ed. Y. Li and X. Ge, Elsevier, 2018, vol. 3, pp. 161–213.
3 R. Briones, L. Serrano and J. Labidi, Valorization of some lignocellulosic agro-industrial residues to obtain biopolyols, *J. Chem. Technol. Biotechnol.*, 2012, **87**(2), 244–249.
4 A. I. Gavrila, A. Vartolomei, I. Calinescu, M. Vinatoru, O. C. Parvulescu, G. Psenovschi, P. Chipurici and A. Trifan, Ultrasound-Assisted Alkaline Pretreatment of Biomass to Enhance the Extraction Yield of Valuable Chemicals, *Agronomy*, 2024, **14**(5), 903.
5 A. O. Ojo, An Overview of Lignocellulose and Its Biotechnological Importance in High-Value Product Production, *Fermentation*, 2023, **9**(11), 990.
6 M. S. T. Amândio, J. M. S. Rocha and A. M. R. B. Xavier, Enzymatic Hydrolysis Strategies for Cellulosic Sugars Production to Obtain Bioethanol from Eucalyptus globulus Bark, *Fermentation*, 2023, **9**(3), 241.
7 V. Oriez, J. Peydecastaing and P.-Y. Pontalier, Lignocellulosic Biomass Fractionation by Mineral Acids and Resulting Extract Purification Processes: Conditions, Yields, and Purities, *Molecules*, 2019, **24**(23), 4273.
8 H. Chen, J. Liu, X. Chang, D. Chen, Y. Xue, P. Liu, H. Lin and S. Han, A review on the pretreatment of lignocellulose for high-value chemicals, *Fuel Process. Technol.*, 2017, **160**, 196–206.
9 A. Toledano, A. García, I. Mondragon and J. Labidi, Lignin separation and fractionation by ultrafiltration, *Sep. Purif. Technol.*, 2010, **71**(1), 38–43.
10 D. Humpert, M. Ebrahimi and P. Czermak, Membrane Technology for the Recovery of Lignin: A Review, *Membranes*, 2016, **6**(3), 42.
11 S. A. Arni, Extraction and isolation methods for lignin separation from sugarcane bagasse: a review, *Ind. Crop. Prod.*, 2018, **115**, 330–339.
12 B. Yan, X. Lin, J. Xiao, Y. Fu and S. Zhang, Comparative study for the separation and depolymerization behavior of lignin from different separation methods, *Fuel*, 2024, **358**, 130145.
13 C. Yang, J. Qin, S. Sun, D. Gao, Y. Fang, G. Chen, C. Tian, C. Bao and S. Zhang, Progress in developing methods for lignin depolymerization and elucidating the associated mechanisms, *Eur. Polym. J.*, 2024, **210**, 112995.
14 M. G. Bontaș, A. Diacon, I. Călinescu and E. Rusen, Lignocellulose Biomass Liquefaction: Process and Applications Development as Polyurethane Foams, *Polymers*, 2023, **15**(3), 563.
15 J. P. S. Aniceto, I. Portugal and C. M. Silva, Biomass-Based Polyols through Oxypropylation Reaction, *ChemSusChem*, 2012, **5**(8), 1358–1368.
16 A. Arevalo-Gallegos, Z. Ahmad, M. Asgher, R. Parra-Saldivar and H. M. N. Iqbal, Lignocellulose: a sustainable material to produce value-added products with a zero waste approach—a review, *Int. J. Biol. Macromol.*, 2017, **99**, 308–318.
17 S. Hu, X. Luo and Y. Li, Polyols and Polyurethanes from the Liquefaction of Lignocellulosic Biomass, *ChemSusChem*, 2014, **7**(1), 66–72.
18 M. Mujtaba, L. Fernandes Fraceto, M. Fazeli, S. Mukherjee, S. M. Savassa, G. Araujo de Medeiros, A. do Espírito Santo Pereira, S. D. Mancini, J. Lipponen and F. Vilaplana, Lignocellulosic biomass from agricultural waste to the circular economy: a review with focus on biofuels, biocomposites and bioplastics, *J. Clean. Prod.*, 2023, **402**, 136815.
19 **https://www.igc.int/en/markets/marketinfo-sd.aspx**, accessed 19/09/2024.
20 P. R. Yaashikaa, P. Senthil Kumar and S. Varjani, Valorization of agro-industrial wastes for biorefinery

process and circular bioeconomy: a critical review, *Bioresour. Technol.*, 2022, **343**, 126126.
21 N. I. Perotti and O. E. Molina, Corn cob as a bacterial substrate for the production of forage protein, *Biol. Waste*, 1988, **26**(2), 125–131.
22 E. Castillo-González, L. De Medina-Salas, M. R. Giraldi-Díaz and C. Sánchez-Noguez, Vermicomposting: A Valorization Alternative for Corn Cob Waste, *Appl. Sci.*, 2021, **11**(12), 5692.
23 P. K. Gandam, M. L. Chinta, N. P. P. Pabbathi, R. R. Baadhe, M. Sharma, V. K. Thakur, G. D. Sharma, J. Ranjitha and V. K. Gupta, Second-generation bioethanol production from corncob – a comprehensive review on pretreatment and bioconversion strategies, including techno-economic and lifecycle perspective, *Ind. Crop. Prod.*, 2022, **186**, 115245.
24 H. Wakudkar and S. Jain, A holistic overview on corn cob biochar: a mini-review, *Waste Manag. Res.*, 2022, **40**(8), 1143–1155.
25 P. K. Gandam, M. L. Chinta, N. P. P. Pabbathi, A. Velidandi, M. Sharma, R. C. Kuhad, M. Tabatabaei, M. Aghbashlo, R. R. Baadhe and V. K. Gupta, Corncob-based biorefinery: a comprehensive review of pretreatment methodologies, and biorefinery platforms, *J. Energy Inst.*, 2022, **101**, 290–308.
26 E. Santolini, M. Bovo, A. Barbaresi, D. Torreggiani and P. Tassinari, Turning Agricultural Wastes into Biomaterials: Assessing the Sustainability of Scenarios of Circular Valorization of Corn Cob in a Life-Cycle Perspective, *Appl. Sci.*, 2021, **11**(14), 6281.
27 J. A. Elegbede, V. A. Ajayi and A. Lateef, Microbial valorization of corncob: novel route for biotechnological products for sustainable bioeconomy, *Environ. Technol. Innovat.*, 2021, **24**, 102073.
28 J. Peyrton and L. Avérous, Structure-properties relationships of cellular materials from biobased polyurethane foams, *Mater. Sci. Eng., R*, 2021, **145**, 100608.
29 A. Kausar, Polyurethane Composite Foams in High-Performance Applications: A Review, *Polym.-Plast. Technol. Eng.*, 2018, **57**(4), 346–369.
30 H. M. C. C. Somarathna, S. N. Raman, D. Mohotti, A. A. Mutalib and K. H. Badri, The use of polyurethane for structural and infrastructural engineering applications: a state-of-the-art review, *Constr. Build. Mater.*, 2018, **190**, 995–1014.
31 M. Ates, S. Karadag, A. A. Eker and B. Eker, Polyurethane foam materials and their industrial applications, *Polym. Int.*, 2022, **71**(10), 1157–1163.
32 G. Tao, J. Yuan, Q. Chen, W. Peng, R. Yu and S. Basack, Chemical stabilization of calcareous sand by polyurethane foam adhesive, *Constr. Build. Mater.*, 2021, **295**, 123609.
33 S. T. Lee and N. S. Ramesh, *Polymeric Foams: Mechanisms and Materials*, CRC Press, 2004.
34 M. C. Iacob, D. Popescu, C. Stochioiu, F. Baciu and A. Hadar, Compressive behavior of thermoplastic polyurethane with an active agent foaming for 3D-printed customized comfort insoles, *Polym. Test.*, 2024, **137**, 108517.
35 D. Dukarska and R. Mirski, Current Trends in the Use of Biomass in the Manufacture of Rigid Polyurethane Foams: A Review, *J. Compos. Sci.*, 2024, **8**(8), 286.
36 P. T. Anastas and J. C. Warner, *Green Chemistry: Theory and Practice*, Oxford University Press, 2000.
37 E. Rusen, G. Toader, A. Diacon, F. M. Dîrloman, L. C. Matache, F. Alexe, A. Dinescu and A. Mocanu, Synthesis and Mechanical Performances of Polyurethane Bio-Based Adhesives Resulted from the Depolymerization of Lignocellulose Biomass, *ACS Omega*, 2023, **8**(41), 38178–38190.
38 H. M. Zabed, S. Akter, J. Yun, G. Zhang, M. Zhao, M. Mofijur, M. K. Awasthi, M. A. Kalam, A. Ragauskas and X. Qi, Towards the sustainable conversion of corn stover into bioenergy and bioproducts through biochemical route: technical, economic and strategic perspectives, *J. Clean. Prod.*, 2023, **400**, 136699.
39 A. C. Mârșolea, A. Mocanu, P. O. Stănescu, O. Brincoveanu, C. Orbeci, R. Irodia, C. Pîrvu, A. Dinescu, C. Bobirica and E. Rusen, Synthesis and characterization of polyurethane flexible foams provided from PET derivatives, fly ash, and glass wastes, *Heliyon*, 2023, **9**(12), e23097.
40 M. Klučáková, Rheological properties of phenolic resin as a liquid matrix precursor for impregnation of carbon–carbon composites with respect to conditions of the densification process, *Compos. Sci. Technol.*, 2004, **64**(7), 1041–1047.
41 R. Mahmood, S. Bilal, A. H. Majeed, I. Khan and E.-S. M. Sherif, A comparative analysis of flow features of Newtonian and power law material: a New configuration, *J. Mater. Res. Technol.*, 2020, **9**(2), 1978–1987.
42 D. J. Jeffrey and A. Acrivos, The rheological properties of suspensions of rigid particles, *AIChE J.*, 1976, **22**(3), 417–432.
43 A. H. Majeed, I. Siddique, A. Mehmood, H. A. Ghazwani, S. Manzoor and S. Ahmad, Finite element simulations of Herschel–Bulkley visco-plastic materials over a cylinder: drag and lift correlation analysis, *Mod. Phys. Lett. B*, 2024, **38**(26), 2450248.
44 P. Kosmela, A. Hejna, K. Formela, J. T. Haponiuk and Ł. Piszczyk, Biopolyols obtained via crude glycerol-based liquefaction of cellulose: their structural, rheological and thermal characterization, *Cellulose*, 2016, **23**(5), 2929–2942.
45 W. Jiang, R. Hosseinpourpia, V. Biziks, S. A. Ahmed, H. Militz and S. Adamopoulos, Preparation of Polyurethane Adhesives from Crude and Purified Liquefied Wood Sawdust, *Polymers*, 2021, **13**(19), 3267.
46 S. Li, W. Li, Q. Zhang, R. Shu, H. Wang, H. Xin and L. Ma, Lignin-first depolymerization of native corn stover with an unsupported MoS2 catalyst, *RSC Adv.*, 2018, **8**(3), 1361–1370.
47 P. Cinelli, I. Anguillesi and A. Lazzeri, Green synthesis of flexible polyurethane foams from liquefied lignin, *Eur. Polym. J.*, 2013, **49**(6), 1174–1184.
48 A. H. D. Abdullah, S. Chalimah, I. Primadona and M. H. G. Hanantyo, Physical and chemical properties of corn, cassava, and potato starchs, *IOP Conf. Ser. Earth Environ. Sci.*, 2018, **160**(1), 012003.
49 U. A. Amran, K. M. Salleh, S. Zakaria, R. Roslan, C. H. Chia, S. N. S. Jaafar, M. S. Sajab and M. Mostapha, Production of Rigid Polyurethane Foams Using Polyol from Liquefied Oil

Palm Biomass: Variation of Isocyanate Indexes, *Polymers*, 2021, **13**(18), 3072.

50 S. Adnan, M. T. I. Tuan Noor, N. H. Ain, K. P. P. Devi, N. S. Mohd, Y. Shoot Kian, Z. B. Idris, I. Campara, C. M. Schiffman, K. Pietrzyk, V. Sendijarevic and I. Sendijarevic, Impact of the hard-segment concentration on highly resilient polyurethane foams based on palm olein polyol, *J. Appl. Polym. Sci.*, 2017, **134**(45), 45440.

51 I. Beverte, U. Cabulis, J. Andersons, M. Kirpluks, V. Skruls and P. Cabulis, Characteristics of Components and Density of Rigid Nanoclay-Filled Medium-Density Polyurethane Foams Produced in a Sealed Mould, *Polymers*, 2023, **15**(15), 3228.

52 I. Beverte, V. Shtrauss, A. Kalpinsh, U. Lomanovskis, U. Cabulis, I. Sevastyanova and S. Gaidukovs, Dielectric Permittivity of Rigid Rapeseed Oil Polyol Polyurethane Biofoams and Petrochemical Foams at Low Frequencies, *J. Renewable Mater.*, 2020, **8**(9), 1151–1170.

53 F. M. de Souza, P. K. Kahol and R. K. Gupta, Introduction to Polyurethane Chemistry, in *Polyurethane Chemistry: Renewable Polyols and Isocyanates*, ACS Symposium Series, 2021, vol. 1380, ch. 1, pp. 1–24.

54 H. U. Meier-Westhues, K. Danielmeier, P. Kruppa; and E. Squiller, *Polyurethanes: Coatings, Adhesives and Sealants*, Vincentz Network, 2019.

55 M. Oliviero, L. Verdolotti, M. Stanzione, M. Lavorgna, S. Iannace, M. Tarello and A. Sorrentino, Bio-based flexible polyurethane foams derived from succinic polyol: mechanical and acoustic performances, *J. Appl. Polym. Sci.*, 2017, **134**(45), 45113.

56 F. C. Alves, V. F. dos Santos, F. M. Monticeli, H. Ornaghi, H. d. S. Barud and D. R. Mulinari, Efficiency of castor oil–based polyurethane foams for oil sorption S10 and S500: influence of porous size and statistical analysis, *Polym. Polym. Compos.*, 2021, **29**(suppl. 9), S1063–S1074.

57 P. Parcheta, E. Głowińska and J. Datta, Effect of bio-based components on the chemical structure, thermal stability and mechanical properties of green thermoplastic polyurethane elastomers, *Eur. Polym. J.*, 2020, **123**, 109422.

58 C. W. H. Rajawasam, O. J. Dodo, M. A. S. N. Weerasinghe, I. O. Raji, S. V. Wanasinghe, D. Konkolewicz and N. De Alwis Watuthanthrige, Educational series: characterizing crosslinked polymer networks, *Polym. Chem.*, 2024, **15**(4), 219–247.

59 W. Chen, F. Lu and N. Winfree, High-strain-rate compressive behavior of a rigid polyurethane foam with various densities, *Exp. Mech.*, 2002, **42**(1), 65–73.

60 K. Liu, W. Liang, F. Ren, J. Ren, F. Wang and H. Ding, The study on compressive mechanical properties of rigid polyurethane grout materials with different densities, *Constr. Build. Mater.*, 2019, **206**, 270–278.

61 B. Li, M. Zhou, W. Huo, D. Cai, P. Qin, H. Cao and T. Tan, Fractionation and oxypropylation of corn-stover lignin for the production of biobased rigid polyurethane foam, *Ind. Crop. Prod.*, 2020, **143**, 111887.

62 K. Gosz, P. Kosmela, A. Hejna, G. Gajowiec and Ł. Piszczyk, Biopolyols obtained via microwave-assisted liquefaction of lignin: structure, rheological, physical and thermal properties, *Wood Sci. Technol.*, 2018, **52**(3), 599–617.

63 L. Jasiūnas, S. T. McKenna, D. Bridžiuvienė and L. Miknius, Mechanical, Thermal Properties and Stability of Rigid Polyurethane Foams Produced with Crude-Glycerol Derived Biomass Biopolyols, *J. Polym. Environ.*, 2020, **28**(5), 1378–1389.